SPE
Society of Petroleum Engineers

SPE 15618

Drag Bit Performance Modeling

by T.M. Warren and A. Sinor, *Amoco Production Co.*
SPE Members

This paper was prepared for presentation at the 61st Annual Technical Conference and Exhibition of the Society of Petroleum Engineers held in New Orleans, LA October 5-8, 1986.

ABSTRACT

Models for the forces required to remove a fixed volume of rock with a single cutter have been applied to different polycrystalline Diamond Compact (PDC) bit designs. The integration of the forces for each cutter over the bit face gives the torque and weight-on-bit (WOB) required for a particular rate-of-penetration (ROP).

This paper presents the results of comparing such a model to laboratory drilling tests for four radically different bit designs in four different rocks. The geometry of each cutter on the bit was determined by detailed measurements of the bit with a 3-axis coordinate measuring machine.

Drilling tests were conducted by "reaming" rock with an 8-1/2" bit that had been previously drilled with a 6-1/4" bit. Only the peripheral cutters engaged the rock during the reaming. Additional tests were conducted where the WOB and torque were recorded while drilling a pilot hole into the top of a flat rock and drilling through two different bed boundaries with constant ROP. The model predictions compared well to the measured data for both the reaming tests and the pilot hole tests.

INTRODUCTION

Analysis of the drilling mechanics of large cutter (greater than 1/4 in. diameter) PDC bits is much easier than that of roller cone bits because of their simpler geometry. At the same time, variations in PDC bit designs result in a wider range of performance than observed with roller cone bits. PDC bit performance is extremely sensitive to formation properties and operating conditions. There is a fine balance between bit durability and designs that ball up in shales. This paper concentrates on the mechanical design parameters for PDC Bits. Bit cleaning considerations are discussed in a companion paper.[1]

The PDC bit model described in this paper was developed to aid bit selection and evaluation. The model also serves as a baseline to identify and quantify additional factors that affect bit performance by comparing model predictions to actual data, either from laboratory or field drilling.

PDC BIT MODEL

The simple kinematics of a large cutter drag bit allows the position of each cutter in space to be easily tracked for a given rotational speed and penetration rate. The exact volume of rock removed by each cutter can be calculated for a given steady state penetration rate because each cutter on the bit remains at a constant position relative to a coordinate system that moves with the bit body.

The PDC bit model is a combination of rigorous geometrical relationships used to describe the kinematics of a particular bit geometry and single cutter force and wear models. The single cutter models predict items such as cutter forces, cutter temperatures, and cutter wear. These predictions are for a single cutter and are independent of the cutter's position on the bit. Appendix 1 discusses the assumptions that were used in the overall model development and Appendix 2 describes the individual force and wear models. Detailed cutter placement information is used to integrate these single cutter models for a specific bit. The method used to generate the cutter location coordinates is discussed in Appendix 3.

Inputs to the model are detailed cutter geometries, formation properties, penetration rate and rotational speed. The model calculates the volume of rock removed by each cutter, total weight-on-bit,

References and illustrations at end of paper.

bit torque, bit imbalance force and total wear flat area. The first step in the model is to calculate the rock removed by each cutter. The effective depth of cut and cut width are then used to calculate the cutter forces. The individual cutter forces and velocities are used to calculate cutter temperature, cutter wear and total bit forces.

Example Model Results

A generic bit design is used as an example to demonstrate the results obtained with the model. The 8-1/2 in. bit is composed of seven 1-1/2 in. cutters arranged on three blades located 120° apart. Figure 1 shows the profile of the bit and the angular location of the cutters on the bit.

Table 1 shows the predicted results for drilling with this bit in Berea Sandstone at 50 ft/hr with a rotary speed of 120 rpm. The cross sectional area of each cutter engaged in the rock, volume of rock removed, resulting force angle, effective side rake and back rake, and velocity of each cutter are shown. These quantities result directly from geometrical considerations and are not influenced by the empirical force models. The circumferential force, axial force, and normal force are calculated for each cutter based on the empirical force models.

Summary data is printed below the individual cutter data. The WOB is the sum of the axial cutter forces and the bit torque is the sum of the circumferential forces times the cutter moment arm. As discussed later, the magnitude and direction (relative to the position of cutter number 1) of the imbalance force is also calculated.

LABORATORY DRILLING TESTS

Laboratory drilling tests were conducted with the four 8-1/2" diameter bits shown in Fig. 2 to provide model validation data and to develop the force functions used in the model. Tests were conducted in Catoosa Shale, Indiana Limestone, Berea Sandstone, and Carthage Marble. The conditions of these tests are discussed in more detail by Warren and Armagost.[1]

Figures 3 and 4 show the lab data and model predictions for three different rocks drilled with bits B and C. Rock strengths of 2.6, 1.2, and .7 were used for the Carthage, Berea, and shale, respectively, for the model results presented in these and following figures. Unless otherwise noted, a bit factor of 1.0 was used. The model for the large cutter bladed bit "C" fit the data for all three rocks very well. Examination of the bit after each test showed no balling on the cutters for any of the rocks when a flow rate of 450 gpm was used.

Good predictions for the flat faced bit were obtained in the Berea and Carthage, but not in the shale. The bit was balled up after the test in shale as discussed in more detail in Ref. 1. The balling caused the calculated ROP to be considerably less than the model predicted. This data for bits B and C indicates that the basic model performance is good as long as the cutters are cleaned.

Figure 5 shows test data and the model predictions (B.F. = .73) for drilling in shale at a range of rotary speeds from 60 to 180 rpm with bit D. The model fits this data very well, but in other cases where poor cutter cleaning is suspected, it has not worked as well for rotary speed response.

The bottomhole pattern was examined for most of the laboratory bit runs. The observed pattern was compared to the model predictions in order to help identify the amount of fracturing that occurs between the cuts made by individual cutters. Figure 6 is a comparison between a bottomhole pattern predicted by the model and the pattern measured with the coordinate measuring machine shown in Appendix 3. In general the patterns show little evidence of fracturing, but often show evidence of off center rotation.

In order to provide a more rigorous test of the model, the 8-1/2 in. bit A was used to ream a previously drilled 6-1/4 in. hole. In this way the forces on the inner cutters were eliminated, while the outer cutters were loaded under the same conditions as if they were drilling. The penetration rate, torque and model predictions (B.F. = 1.22) for both drilling and reaming are shown in Fig. 7. The bit removed only 41% as much rock volume while reaming as compared to that removed while drilling. The model predictions of both torque and WOB were slightly low for the reaming case. This probably is due to a higher relative imbalance force during reaming than during drilling. The reaming tests were also conducted in Berea and with a different bit in Carthage with similar results.

During several tests the WOB and torque were recorded while drilling a pilot hole into the top of a flat rock at a constant penetration rate. Figure 8 shows two sets of data for drilling with bit D into the top of a Berea core and into a shale core. This data tested the model as an increasing number of cutters engage the rock. The predicted torque and weight agrees reasonably well with the observed values.

Cutter Removal Tests

Cutters were removed from a sharp bit similar to bit B to examine the effect of cutter interaction on the bit performance. As cutters are removed from a bit, adjacent cutters must remove more rock in order to maintain the penetration rate. The objective of the cutter removal tests was to systematically increase the rock removed by the remaining bit cutters and observe the change in bit loading required to drill at various rates. The cutters were removed in groups of four. Figure 9 shows the cutter profile at the beginning, end, and two intermediate stages of the test. At the end of the test only the minimum number of cutters required to cut the hole bottom were remaining. Figure 10 shows schematically the objective of these tests. Reference 1 contains a description of the tests.

The cutter removal tests show that there is a negligible effect of cutter interaction on the cutter forces required to drill Carthage Limestone as indicated by Fig. 11. At the higher WOB there was a very slight increase in penetration rate for a

given WOB. Similar results were obtained for the bit torque in Carthage and for both ROP and torque in Indiana Limestone.

Figure 12 shows the calculated vertical load on the same ten cutters on the bit before removing any cutters and after removing 29 cutters. The cutter force is much greater for the peripheral cutters after removing 29 cutters even though the penetration rate is not immediately affected. The change in load is caused by a change in the volume of rock removed and by a change in the effective back rake. For example, the ninth cutter originally had a cutting area of 0.0122 in^2 and an effective back rake of -19 deg. After removing 29 cutters, this cutter had a cutting area of 0.0475 in^2 and an effective back rake of -6.7 deg. The increase in cutting area tended to increase the cutter load but the decrease in effective back rake tended to reduce the cutter load by 40%. The combination of high cutter load and high linear velocity of the peripheral cutters will severely accelerate the wear of these cutters.

Tests with Worn Bits

Tests were conducted with a moderately worn bit similar to bit B to compare the penetration rate for sharp and worn cutters in several rocks. The worn bit had a total wear flat area of 2.48 $in.^2$ after having drilled 1020 ft in 170 hrs (6 ft/hr). The diamond layer was worn even with the carbide wear flats. This is typical of bits worn in hard rocks.

Figure 13 shows a comparison between the model predictions and experimental data for both the sharp and worn bits while drilling Berea and Carthage. The effect of bit wear is accounted for in the model by adding the normal force due to cutting and a load supported on the wear flat. The entire wear flat area was assumed to be in contact with the rock in this example.

Many field dulled bits show the carbide backing to be worn below the diamond layer. For these cases the entire wear flat area is not in contact with the formation and does not impede the drilling rate as severely as the example shown in Fig. 13.

Cutter removal tests were conducted with the moderately worn bit used in the tests described above. These test were conducted in the same manner as those used with the sharp bit. Figure 14 shows the penetration rate steadily increasing as the cutters were removed. The model predicts an increase in penetration rate, but not the steep rate of increase that was observed experimentally.

CUTTER FORCE BALANCE

It is generally recognized in the drag bit industry that the forces acting on a drag bit should be balanced. It is not clear that this is totally accomplished in many commercial bit designs, nor is it clear that a uniform definition of "force balance" is used.

The cutter force components in a plane normal to the bit axis can be resolved into a moment about the bit centerline and a radial force. The moment is simply the bit torque and the radial force is the imbalance. This imbalance force is oriented in a fixed direction relative to the bit face. It tends to push the bit into the wall of the hole as the bit rotates. The results of force imbalance in some cases can be seen in laboratory drilling by the existence of an over gauge hole.

If the forces are not balanced, the bit tends to rotate off center resulting in accelerated wear and reduced penetration rate. The large full-gauge stabilizer sections on bits tend to counteract the imbalanced cutting forces and cause the bit to rotate around its centerline.

There are several sources of bit imbalancing forces. For bits with a tapered profile, the normal force on the cutters can be resolved into a vertical force (WOB component) and a radial component as shown in Fig. 15. The vectorial sum of the radial components for all the cutters generates one potential for a force imbalance. A second source of imbalance is a nonzero vectorial sum of the circumferential cutting forces acting on all the cutters.

The two sources of imbalance discussed above can be computed with the PDC model because they rely only on basic physics, geometry, and the cutting force models. A third source of imbalance is due to cutter side rake. Prediction of single cutter sideforces caused by side rake are limited due to scarce experimental measurements.[3,4] Unlike the penetrating force and cutting force, the effect of sideforce cannot be evaluated indirectly from drilling tests unless a method is available to measure the bit sideforce generated at the cutters. This force is resisted by the stabilizer contact force; thus, any measurements must be made at the stabilizer/rock interface and, therefore are impractical. In this paper, the effect of side rake is neglected, but it is recognized as a potential source of error. It is doubtful that an imbalance force caused by this effect would counteract the imbalance due to the other two sources, thus the imbalance force calculations are conservative.

A bit may also be imbalanced due to its mass distribution, but this is insignificant at normal rotary drilling speeds. In cases where the bit is run on a turbine, the mass balance may be significant.

The generic bit used in the previous example to demonstrate the PDC model operation has an imbalance force of 2180 lb (at the specified operating conditions) which is 42% of the applied WOB. Without stabilization the bit would rotate off center and drill a 9.3 in. diameter hole. This assumes that the bit rotates so that the resulting side loading is reduced to zero.

The cutters on the bit can be relocated to reduce the imbalance force. Repositioning blade 3 from its position at 240° from blade 1 to 210° reduces the imbalance force to 30 lb.

Bit C was used to drill a core that had been prepared to test bit response at bed boundaries. The top half of the core was Berea sandstone and the bottoms half was the stronger Carthage marble. Figure 16 shows that the initial WOB and torque are

higher than expected for this bit. This occurs because the small number of cutters on the bit provide poor bit stabilization as the bit drills into the top of the core. The calculated imbalance force is only 218 lb for the conditions used, but this is sufficient to cause the hole to be drilled slightly over gauge before the stabilizer pads engage the rock. Figure 17 shows the calipered hole diameter for this test and Fig. 18 shows the bit dimensions. Notice that the length of over gauge hole coincides with the distance from the first gage cutter to the diamond stabilizer section on the bit. After the stabilizer pads engaged the rock, the differences between the predicted and observed WOB and torque are much less.

The hole was nearly gage while drilling the Berea until the nose cutter of the bit hit the harder Carthage rock. The bit was considerably unbalanced as it drilled through the Berea/Carthage boundary. The calculated imbalance force increased from 200 lb while drilling all Berea to a maximum of 730 lb when the nose cutter was 1/2 in. into the Carthage and then gradually decreased to a value of 437 lb while drilling only Carthage. This imbalance was sufficient to cause the stabilizer pads on the bit to cut the Berea hole 0.2 in. over gauge. The hole diameter in the Carthage gradually decreased as the stabilizer pads entered the top of the Carthage.

The model predictions shown in Fig. 16 qualitatively track the increase in WOB and torque as the bit drills across the bed boundary, but the actual measured values are about 50% higher than the model predictions. The values are also higher than the stabilized values taken from the performance tests with the bit while drilling in other Berea and Carthage rocks (these values are included in Fig. 16). It is apparent that the test was stopped (due to reaching maximum allowable drilling depth) before the WOB and torque returned to their stabilized values for drilling in Carthage at 20 ft/hr.

The predicted WOB and torque for bit D while drilling a pilot hole was more correct (Fig. 8) than for drilling with bit C (Fig. 16). The WOB and torque for bit D did not overshoot the stabilized values as they did for bit C. Bit D provided a more balanced cutting action with 6 blades and small cutters when only a fraction of the bit face was buried than bit did C

The above tests indicate that the weight and torque required to drill at a fixed penetration rate when the bit is unbalanced, as indicated by the over gauge hole, are much higher than those required when the bit is operating in a stabilized condition. This phenomenon has been observed several times in the laboratory. It implies that the model predicted penetration rate is too high if the bit drills in an unstable mode.

The above discussion describes a mechanism that causes a balanced bit design to drill unstably as it drills across bed boundaries. Even for the case of drilling homogeneous rock, the bit imbalance force will change as the penetration rate changes. An unstable drilling condition can also be caused by poor bit design or by manufacturing imperfections.

From a bit design standpoint, the cutters must not only be placed to minimize imbalance but to equalize wear on the cutters (see Ref. 2 for criteria for equal wear). Additionally, the cutters must be located so that the bit can; 1) be manufactured with ease and reliability, 2) maintain structural integrity, and 3) be cleaned by the drilling fluid. Thus any practical bit design is a compromise between the solutions for several different problems.

MANUFACTURING DEFECTS

Figure 19 shows the initial tests with bit D when it was first run as a new bit. Even though the bit drilled a nearly gauge hole, the bottom hole pattern showed a distinct seven lobe pattern, rather than a smooth circular pattern. The penetration rate with the bit increased by a factor of 2 to 3 after drilling with the bit in Carthage, as indicated by the later tests in Fig. 19. This change occurred after drilling only a few feet under laboratory conditions. Several additional tests were run to confirm the penetration rate improvement and to identify the cause of the performance improvement. After these tests were completed, it was apparent that the backup material behind several of the cutters was rubbing on the formation. Wear flats had begun to develop even though the diamond layer was not worn at all. This can be seen in the photograph of one of the worn cutters shown in Fig. 20.

The low initial penetration rate observed with the new bit was caused by the carbide cutter backing rubbing against the formation. This caused the bit to chatter until the protrusion was worn away.

Figure 21 shows the measured profile of the bit in the area of the defective cutters. Apparently the bit was manufactured with several cutters set at an incorrect angle. This allowed the carbide behind the cutter to engage the rock. After running the bit a short time the carbide wore away and the bit performance significantly improved.

The defect discussed in the above bit may have resulted in only a short duration superficial reduction in bit performance or it may have had more serious repercussions if the bit had been run in the field. Heat checking in the carbide material supporting the low cutters was obvious, even in the short time the bit was run in the laboratory. This could easily cause a transverse fracture in the backup carbide and result in the loss of the cutter. The loss of a single cutter in the location of the defect probably would cause the bit to ring out and fail prematurely.

SIMULATIONS FOR DRILLING LAYERED ROCK

The PDC bit model was used to simulate drilling through a bed boundary with an 8-1/2 in. tapered bit profile like that shown by bit C in Fig. 2. Cases were run for drilling from a rock similar in strength to Berea sandstone into a rock similar to Carthage Limestone. Figure 22 shows the change in normal load on three cutters on the bit as it passes through the bed boundary. The cutters are the same

ones shown in Fig. 18. The distance shown on the plot is the position of the nose of the bit.

For the case of drilling from soft to hard, it is assumed that the bit is being run at 120 rpm and drilling at 120 ft/hr. The WOB is maintained at 10,000 lb while drilling across the bed boundary. The predicted penetration rate rapidly decreases from 120 ft/hr to 45 ft/hr. The cutter forces shown in Fig. 22 are steady state calculations and probably are very conservative. As shown in laboratory drilling tests the actual WOB and torque may be 30 to 50% higher than the steady state predictions. Additionally there could be significant impact loading of the cutters. These loads can be sufficient to severely chip the cutters and in some cases break the whole cutter away from the bit body.

For the case of drilling from hard to soft, it is assumed that the initial WOB is increased to 15,000 lb after the hard layer is encountered in order to increase the penetration rate. This significantly increases the loading on the cutters. The calculated forces are shown in Fig. 23 as the bit drills through the boundary between hard rock to softer material. The penetration rate increases from 75 ft/hr to 185 ft/hr as the bit passes the boundary.

Comparison of the two cases above indicate that drilling from hard to soft may be more detrimental to the bit than the opposite. The imbalance condition is higher and is maintained for a longer time period. The laboratory tests have shown that the total bit loading predicted by the model is very conservative. Individual cutter loading in excess of that shown in Fig. 23 is expected. These cases indicate that for the particular bit used in the calculations, the middle cutter on the blade is more likely to be damaged than either the nose or gage cutter.

Laboratory drilling tests with a bit similar to the one used in these simulations show the bit has excellent performance in soft rocks and does not ball up in shale, but these simulations point out that the bit may be susceptible to damage when drilling non-homogeneous rock. They also indicate that if an unexpected hard streak is encountered while drilling with a bit of this type the best procedure is to refrain from increasing the WOB to protect the bit as it comes out the bottom of the hard streak.

CUTTER BALLING

The penetration rate performance of the flat-faced bits in Indiana limestone appeared as if the bits were balled up, but there was little visual evidence of bit balling at the end of the tests. Figure 24 shows a typical penetration rate response curve obtained with bit B. It appears that the limestone material packs in front of the cutters and decreases the penetration rate by the combined effect of supporting the cutter load and confining the rock as shown schematically in Fig. 25. This is surmised from the reduced rate of increase in penetration rate as the WOB is increased.

The force model can be made to predict the correct ROP as shown in Fig. 24 by assuming that the rock debris confines the rock in front of the cutter, increasing its effective strength. This increase in strength is assumed to be a function of the depth of cut. The effective rock strength function for each condition is included in Fig. 24. At low WOB the rock strength is unaffected, but at high WOB the effective rock strength is a function of both depth of cut and the hydraulic energy. For example, the effective rock strength at 10 Klb WOB is 1.7 at 420 gpm and is 2.3 at 280 gpm rather than the original value of 1.2. Unfortunately, there is no mechanism in the model to decide when to apply this phenomenon. Consequently this portion of the model can be used to match observed data, but has little predictive capability until a mechanism is included to predict imperfect cutter cleaning.

SUMMARY

A model for PDC bits has been developed and confirmed by laboratory tests. The program is useful for evaluating the mechanical design of a particular bit. The model is based on static cutter force calculations. In many cases the actual cutter loads are higher than those calculated by the model or conversely the penetration rate is lower than expected at a particular applied load.

Laboratory tests have demonstrated the adverse affect of imbalanced bit loading on the penetration rate and bit torque. These tests have pointed out the detrimental effect of seemingly minor manufacturing defects in cutter placement.

The rapidly changing cutter loading and the increased imbalance loads while drilling through dissimilar materials have been demonstrated. The practice of increasing WOB to maintain penetration rate in a hard streak may be counter productive if the bit is damaged when it exits the hard layer.

NOMENCLATURE

d_c = depth of cut per revolution, in.
R^c = rate of penetration, ft./hr.
N = rotary speed, rpm
Θ = radial location of the cutters
RS = relative rock strength
F_N = normal Force on cutter, lbs.
α^N = angle of internal friction of the rock, deg.
BR = cutter back rake, deg.
d_w = width of cut, in.
d^{ce} = effective depth of cut, in.
B_f = Bit Factor
A^w = Average cutter wear rate, in^2
F_x = horizontal Force on cutter, lbs.
d^{cm} = mean depth of cut, in.
β = Force angle relative to the axis of the bit and the normal force, deg.
T_w = mean wearflat temperature on PDC cutter, $^\circ C$
T_{f1} = cooling fluid temperature, $^\circ C$
K_{hF} = rock formation thermal conductivity, $w/cm/^\circ C$
K_f = cutter/rock friction coefficient
V = cutting speed, m/s
f = thermal response function, $^\circ C\ cm^2/W$
α_f = rock formation thermal diffusivity, cm/s
L = cutter wearflat length, cm.
C_1, C_2, C_3, C_4 = Constants

REFERENCES

1. Warren, T. M. and Armagost, W. K.: "Laboratory Drilling Performance of PDC Bits," SPE 15618, Presented at the 1986 Annual Technical Conference and Exhibition, New Orleans, Oct. 5-8, 1986.

2. Glowka, David A.: "Implications of Thermal Wear Phenomena for PDC Bit Design and Operation," SPE 14222, Presented at 60th Annual Technical Conference and Exhibition, Las Vegas, Nevada, Sept. 22-25, 1985.

3. Melaugh, J. F., and Salzer, J. A.,: "Development of a Predictive Model for Drilling Pressurized Shale with Stratapax Blank Bits," ASME Energy Technical Conference, Houston, Texas, Jan. 19-22, 1981.

4. Huang, Hsin I., and Iverson, Robert I.: "The Positive Effects of Siderake in Oilfield Bits Using Polycrystalline Diamond Compact Cutters," SPE 10150, Presented at the 56th Annual Technical Conference and Exhibition, San Antonio, Texas, Oct. 5-7, 1981.

5. Cheatam, J. B., Jr. and Daniels, W. H.: "A Study of Factors Influencing the Drillability of Shales: Single-Cutter Experiments with STRATAPAX Drill Blanks," J. Energy Res. Tech., Vol 101 (Sept. 1979) 189-195.

6. Thomsen, E. G., Yang, C. T. and Kobayoshi, S.: Mechanics of Plastic Deformation in Metal Processing, The MacMillian Co., New York, 1965.

7. Gray, K. E.: "Fixed Blade Planing of Rock," Ph.D. Dissertation, University of Texas, 1962.

8. Warren, T. M.: "Penetration Rate Performance of Roller Cone Bits," SPE 13259, Presented at the 59th Annual Technical Conference, Houston, Sept. 16-19, 1984.

9. Glowka, D. A. and Stone, C. M.: "Thermal Responses of Polycrystalline Diamond Compact Cutters Under Simulated Downhole Conditions," Soc. Pet. Engr. J. (April 1985) 143-156.

10. Ortega, A. and Glowka, D. A.: "Frictional Heating and Convective Cooling of Polycrystalline Diamond Drag Tools During Rock Cutting," Soc. Pet. Engr. J. (April 1984) 121-128.

11. Zijsling, D. H.: "Analysis of Temperature Distribution and Performance of Polycrystalline Diamond Compact Bits Under Field Drilling Conditions," SPE 13260, Presented at the 59th Annual Technical Conference and Exhibition, Houston, Sept. 16-19, 1984.

12. Hibbs, Jr., L. E., and Flom, D. G.: "Diamond Compact Cutter Studies for Geothermal Bit Design," ASME Journal of Pressure Vessel Technology, V100, Nov. 1978, 406-416.

ACKNOWLEDGEMENTS

We wish to thank Diamant Boart U.S.A., Inc., Norton-Christensen, Inc., and Strata Bit Corporation for providing bits used in the testing program.

APPENDIX 1 - MODEL ASSUMPTIONS

The PDC bit model is based on several assumptions about the mechanics of drag bit drilling which simplify the model development.

The bit body and cutters are considered to act as a rigid body and the bit loading is assumed to be static. This assumption allows the utilization of a two dimensional formation model rather than a three dimensional model. The validity of this assumption for laboratory drilling is largely determined by the particular bit design. Static bit loading is a good assumption when the bit has balanced cutting forces, but for imbalanced bits the loading is not static. Drillstring dynamics may result in dynamic bit loading for field drilling.

The cutters are assumed to make a smooth cut at the boundary of the cutter and there is no breakout between cuts. Single cutter tests have produced cuts that have a cross-sectional geometry almost identical to the cutter. Examination of the bottomhole pattern for several different bit types shows this to generally be true, except cases where two adjacent cutters leave a narrow ridge of unsupported rock. In this case fracturing between cuts will occur. The validity of the smooth cut assumption should be better for ductile rocks than for brittle rocks, but attempts to incorporate rock failure outside the cutter boundary have provided no significant improvement to the model predictions.

It is assumed that the failed rock does not contribute to the cutter forces. This assumption is not valid for rocks, bit designs, and hydraulic conditions where bit balling occurs. It appears to be valid for all the Carthage Limestone and Berea Sandstone and some of the shale tests included in this paper.

It is assumed that the bit rotates about its centerline, but the bit centerline may precess around the hole center line, thus drilling a hole larger than the bit diameter. In many cases the bit centerline does not correspond to the hole centerline because of imbalanced cutting forces acting on the bit. The potential for this to occur can be detected with the model, and the results of a specific off center rotation on the imbalanced force can be calculated, but the amount of off-center rotation can not be directly determined.

APPENDIX 2 - CUTTER FORCE AND WEAR MODELS

Several references in the literature discuss both theoretical and empirical cutter force models. Cheatham[5] has shown that the cutter forces are functions of the cutting area and rock shear strength. His tests indicate that the cutter forces are independent of the particular cutter shape and can be predicted with Merchant's[6] metal cutting model. Data published by Gray[7] shows that the incremental

force required to penetrate rock decreases with the depth of cut. His data and numerous other references show that the normal force is a function of the back rake.[5,3] The cutting force also seems to be independent of the side rake of the cutter.[3]

These observations are incorporated in the current model and seem to be justified by later experiments. The cutter force function used in the PDC model was empirically developed from laboratory data for full scale bits. It is written in terms of a "relative rock strength" used in a roller cone bit model.[8] This rock strength is generally calculated from drilling data but it is approximately proportional to the compressive strength of the rock.

The effect of cutter back rake is based on the Merchant metal machining model. The effect of the variation in depth of cut on the penetrating force is given by the function for effective depth of cut shown in Fig. 26. This function is based on an empirical fit to laboratory drilling data in Carthage Marble, Berea sandstone, and Catoosa shale. It probably varies slightly with the rock properties, but is considered constant with sufficient accuracy for the results presented in this paper.

Combining the effects discussed above results in a normal cutter force given by

$$F_N = \frac{\cos(\alpha - BR)}{1-\sin(\alpha-BR)} \cdot dw \cdot B_F \cdot RS \cdot d_{ce} \cdot C_1 + A_w \cdot RS \cdot C_2 \quad ..(1)$$

Equation 1 includes a bit factor term, B_F, to account for unexplained effects for a particular bit. A value of this factor greater than 1.0 indicates that the bit drills slower than expected and a value less than 1.0 indicates that the bit drills faster than expected. For the bits reported in this paper the bit factors ranged from .75 to 1.22, indicating that the model predicted the forces within 25% of the measured values without the use of the bit factor.

The circumferential cutter force is dependent on both sliding friction between the cutter and rock and the force required to fracture the rock. It is given as

$$F_X = \frac{\sin(\alpha - BR)}{1-\sin(\alpha-BR)} \cdot C_3 \cdot RS \cdot d_w \cdot d_{cm} + C_4 \cdot F_N \quad ....(2)$$

The first term of this equation is the cutting force and the second term is the nonproductive friction carried on the cutter wear flat.

In general, a cutter does not contact the rock on a surface normal to the axis of bit rotation. Figure 15 is a schematic of a cutter positioned so that it cuts at an angle, β, relative to the axis of the bit. The penetrating force is assumed to act normal to the cut and its direction is determined from the geometry of the cut. The vertical component of the penetrating force is given by

$$F_V = F_N \cdot \cos(\beta) \quad .....(3)$$

The weight-on-bit is the sum of the vertical components of the penetrating force. For a flat-faced bit the WOB is nearly equal to the sum of the penetrating forces but for a tapered profile bit the WOB may be considerably less than the penetrating force. This results in a tapered bit requiring less WOB than a flat-faced bit to drill at the same ROP. For both bits the penetrating force is the same and the resulting wear is similar, assuming the same number and size of cutters in both cases.

The back rake and side rake of a cutter are defined and measured on the bit as if the cutter makes a cut on a horizontal surface. In practice the cutting surface for any particular cutter on a bit may be oriented at any angle between horizontal and vertical. An effective back rake and side rake are calculated relative to the actual cutting plane. The effective back rake and side rake are used in the force and wear models.

Laboratory drilling data was used to refine the force functions after the geometry portion of the code was developed so that the rock removal by each cutter could be calculated. It is assumed that if a particular force function can be integrated over all the cutters on the bit to give the correct WOB and torque, then the force on individual cutters is correct. The Merchant[6] machining model was used as the starting point to develop the particular force models discussed above. Laboratory drilling data from several bits was used to develop the empirical force model coefficients.

Glowka[2] discusses the wear mechanisms for PDC bits and their dependence on cutter temperature. His temperature model along[9,10] with an empirical wear function has been incorporated into the model discussed in this paper. The cutter temperature is estimated from the following relationship.

$$T_w = T_f + \frac{K_f F_N V F}{A_w} \left[1 + \frac{3\sqrt{\pi}}{4} f K_{hF} \left(\frac{V}{\alpha_L L}\right)^{1/2}\right]^{-1} ..(4)$$

The wear rate is based on an empirical relationship between wear rate in Jack Fork sandstone and cutter temperature.[12] A relative formation abrasiveness is used to relate the wear rate for Jack Fork sandstone to the particular rock being drilled. The wear rate is converted to height worn off the cutter and the cutter geometry is modified for wear once every 15 minutes of simulated drilling.

APPENDIX 3 - BIT GEOMETRY MEASUREMENT

A detailed description of the bit geometry is needed to run the PDC model. This description is determined by measurements with a three axis coordinate measuring machine. Figure 27 is a photograph of this machine in use.

The bit is mounted in a machinist rotary table and positioned so that the measurements for each cutter can be made approximately normal to the cutter face. Measurements are also taken to locate the center of rotation of the bit. The three Cartesian coordinates and the angular position of the bit are recorded for each cutter at 4 to 12 points along the edge of the diamond surface.

The cutter measurements are processed through a geometry code to increase the coordinate density by interpolating between the points measured on the cutter by either linear or circular arc interpolation, depending on a connectivity code that is recorded with the points. These coordinates are referenced to the bit centerline and a bit height datum. The side rake and back rake of each cutter is determined. Figure 28 is a general schematic of the geometry generation process.

A plot of the cutter profile is made as a quality control step after the data is processed. Any gross mistakes in the measurements can be identified in this step. Frequently mistakes made during the bit manufacturing process are also discovered.

It is not unusual to find that the pin on a bit is misaligned with the bit face by as much as .015 in. or that cutter protrudes from the bit profile more than it should. Both of the above problems may be short lived and eliminated with only a slight amount of wear on the bit or, depending on their severity, they may result in significantly reduced bit performance.

APPENDIX 4 - CUTTER INTEGRATION

Each cutter on a PDC bit moves in a spiral path which has a radius equal to the distance from the bit centerline to the cutter and a pitch equal to the distance given by the penetration per revolution. Under steady-state drilling conditions, the forces acting on a cutter and the volume of rock removed by it are constant during one bit revolution. The model calculations are required only as each cutter passes a formation reference plane. Figure 29 shows a rock sample with the reference plane used for the calculations crosshatched. The formation surface is specified only on this crosshatched, positive radial-vertical plane. The rock surface on the reference plane is divided into elements by a series of vertical grid lines with a spacing small enough to give sufficient detail to the bottom hole profile (typically 0.01 in.).

The bit cutters are specified with radial, vertical, and angular coordinates with points located at the same grid spacing used for the formation elements.

This fixed grid system allows the radial coordinates of the bit cutters and formation to be specified with integer subscripts to minimize computer storage requirements and simplify the computational scheme. The actual bottomhole geometry is described as the distance above a formation datum at each grid line. The bit cutting surface is described by a similar process relative to the bit body datum.

Figure 30 shows an example of a portion of the bit and bottom hole described with the fixed grid system. Any rock that extends above a cutter is removed by setting the formation grid points equal to the bit grid points. In this example one cutter passes above the formation surface and removes no rock while the other cutter removes the shaded rock area.

The bit is rotated one revolution with each cutter removing rock to initialize the bottomhole profile. This must be done at the same penetration rate as used for the force calculations because the bottom hole profile is dependent on the advancement rate. During this step, no force or bit wear is calculated. The bit rotation is divided into irregular steps dictated by the angular position of the cutters on the bit. At each step the bit body datum is moved toward the formation datum a distance given by

$$d = rop/rpm * (\theta_i - \theta_{i+1}) \quad \text{.....(5)}$$

and the formation is set even with the cutters that are positioned at the reference plane. In this way the bottom hole reference plane is initialized to the pattern dictated by the bit geometry and advancement rate.

The bit is then rotated a second revolution, again with stops made as each cutter passes the reference plane. The rock removed by each cutter is calculated, cutter forces and wear calculated, and the bottomhole pattern altered to reflect the rock removed.

TABLE 1. EXAMPLE OUTPUT FROM PDC MODEL

CUTTER NO	AREA OF CUT	VOLUME OF CUT	FORCE ANGLE	CIRC. FORCE LB	VERT. FORCE LB	NORMAL FORCE LB	VELOCITY M/S	EFFECTIVE SIDE RAKE	EFFECTIVE BACK RAKE
1	0.0947	0.3804	-13.8	1359.	1398.	1440.	0.21	-14.2	-9.1
2	0.0470	0.9957	41.6	946.	648.	867.	1.08	-10.0	-16.3
3	0.0174	0.4543	55.1	448.	268.	469.	1.32	-12.7	-14.1
4	0.0699	0.1728	27.8	1558.	1135.	1284.	0.85	-12.3	-19.2
5	0.0039	0.1006	48.2	85.	67.	101.	1.31	-17.9	-16.6
6	0.0868	0.9426	16.3	1436.	1280.	1333.	0.55	-11.9	-14.5
7	0.0293	0.7046	51.1	601.	356.	567.	1.23	-10.0	-16.5

ROTARY SPEED = 120. RPM.
PENETRATION RATE = 50. FT/HR
ROTATING TIME = 0. HR.
IMBALANCE FORCE = 2180. LB.
IMB. FORCE ANGLE = 189. DEG.
WEIGHT-ON-BIT = 5153. LB.
BIT TORQUE = 1271. FT-LB.

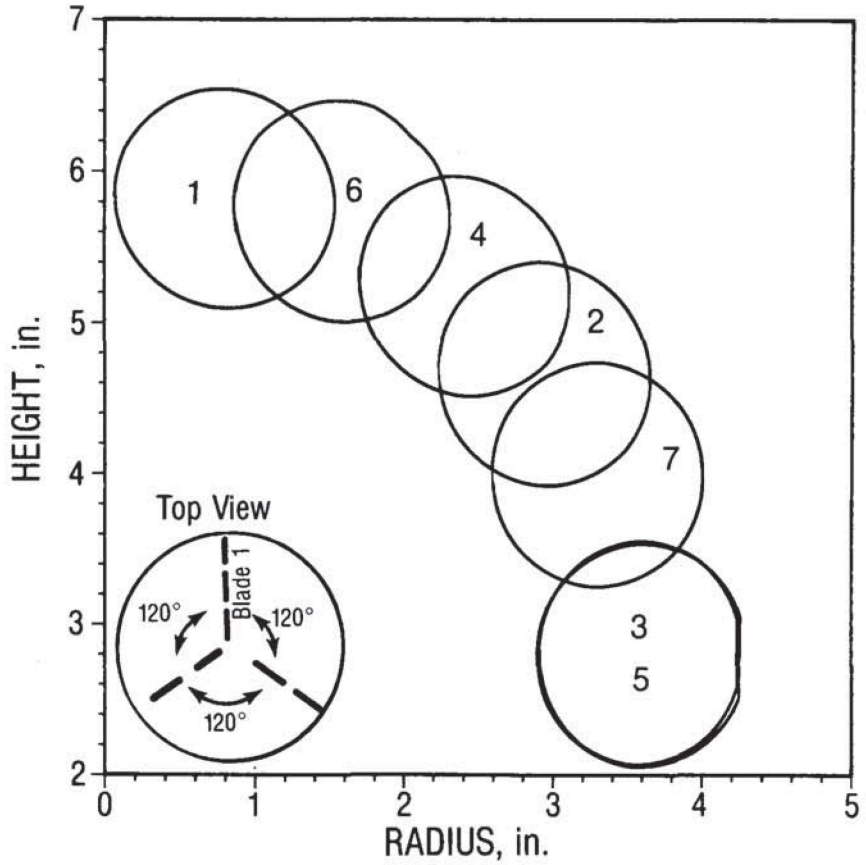

Fig. 1—Profile of cutters on demonstration bit used in example calculations.

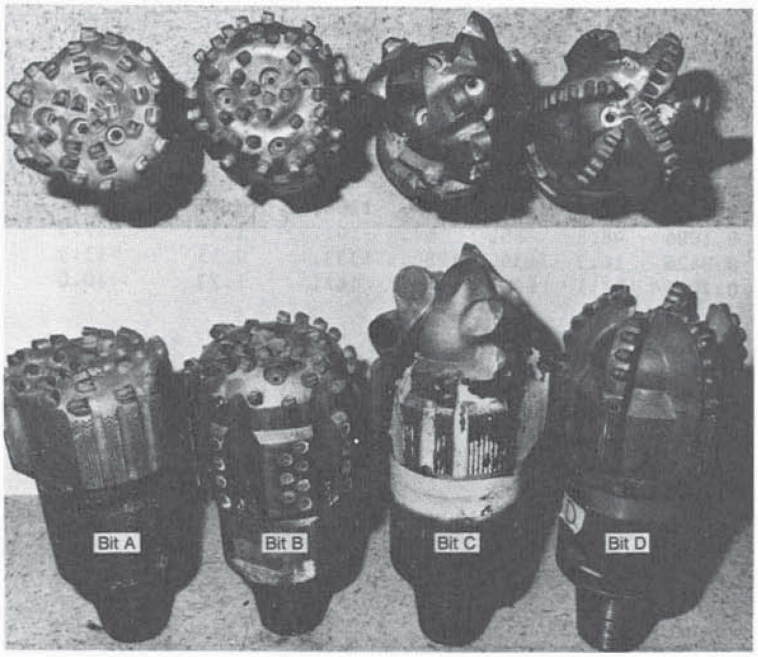

Fig. 2—Photographs of 8.5-in. bits used in test program.

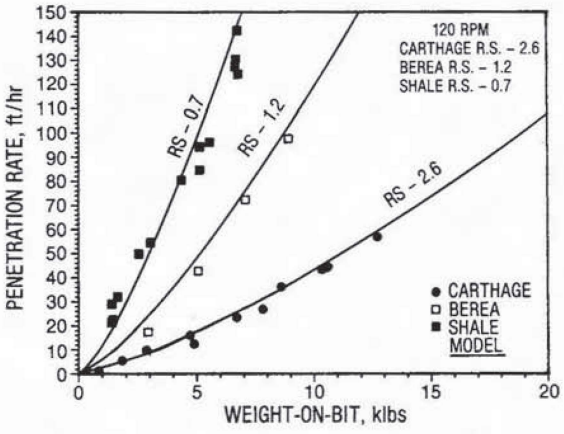

Fig. 3—Comparison of model predictions and laboratory data for Bit C.

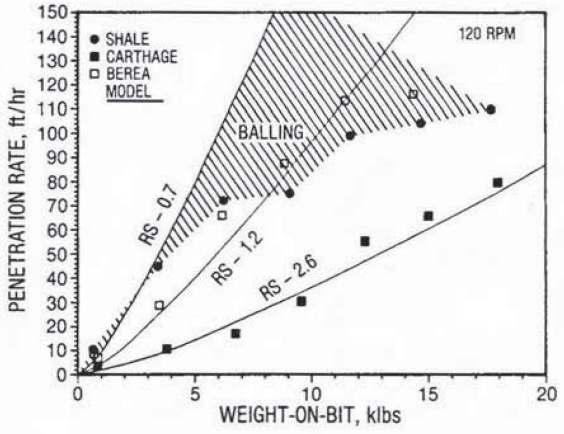

Fig. 4—Comparison of model predictions and laboratory data for Bit B.

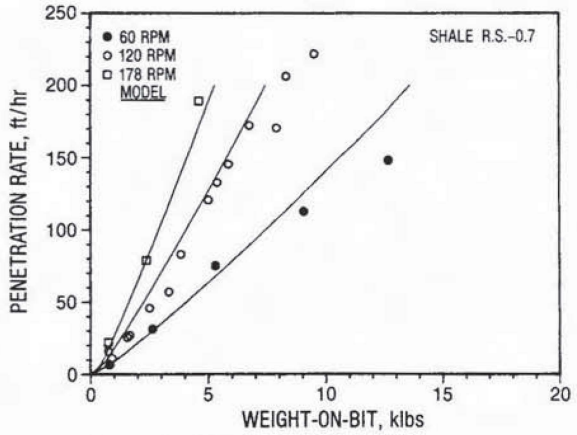

Fig. 5—Rotary speed response of Bit D.

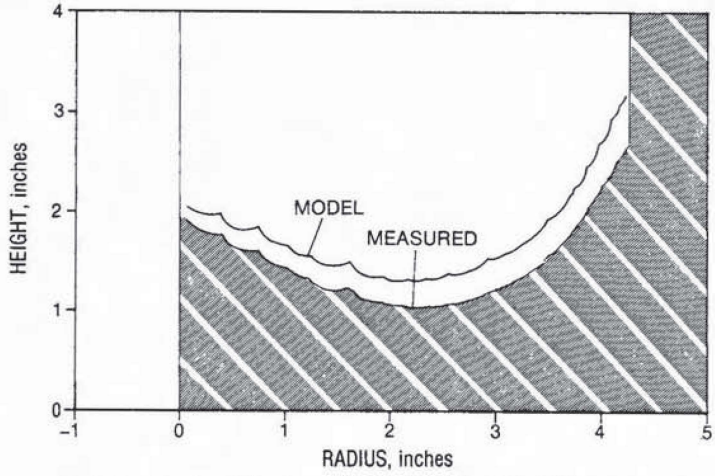

Fig. 6—Comparison of predicted and measured bottomhole profile for Bit B with eight cutters removed.

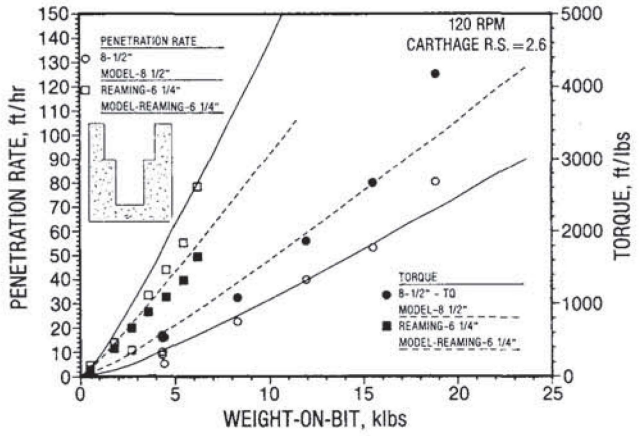

Fig. 7—Comparison of drilling vs. reaming data for Bit A.

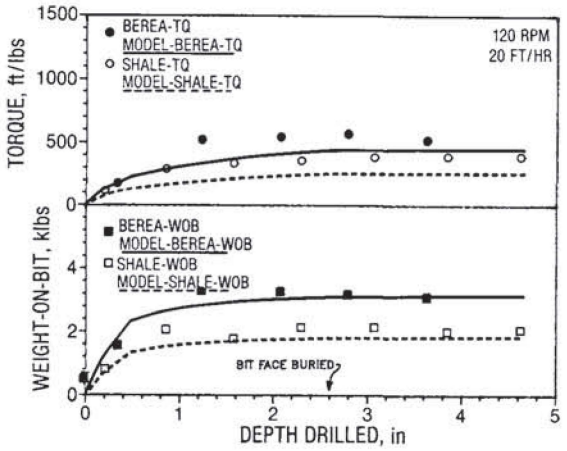

Fig. 8—Data measured and predicted while drilling pilot hole in Berea and shale core with Bit D.

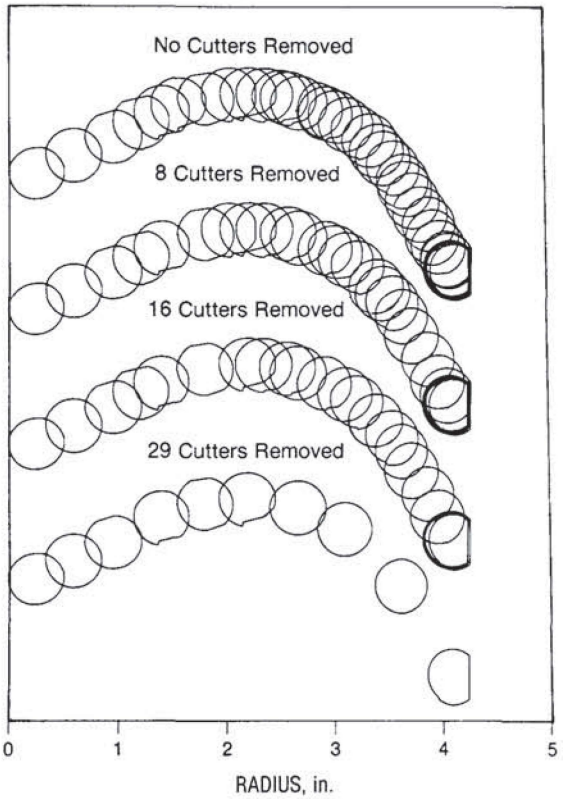

Fig. 9—Cutter profile at various stages of cutter removal tests.

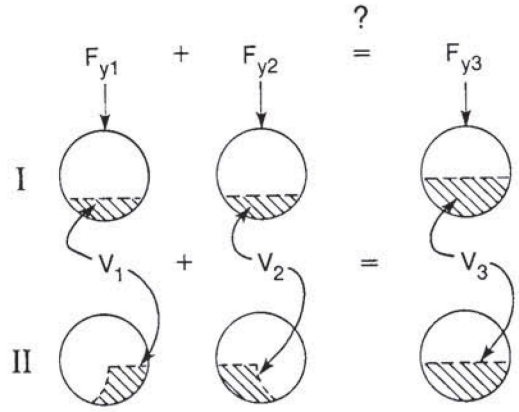

Fig. 10—Schematic of cutter removal test objective.

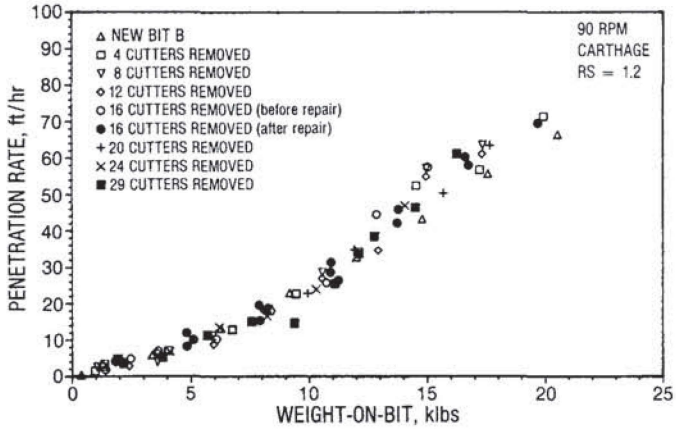

Fig. 11—Penetration rate in Carthage limestone for cutter removal test.

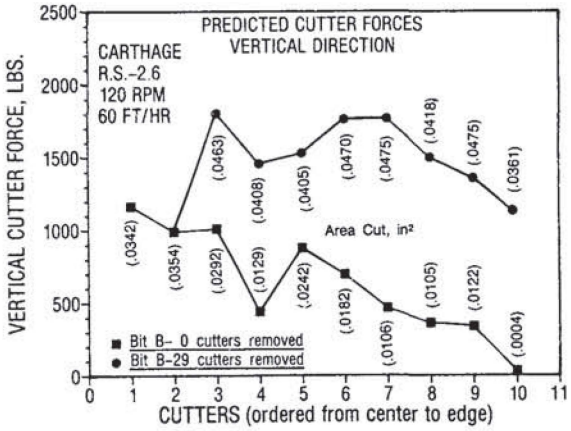

Fig. 12—Normal force on cutters before and after 29 cutters were removed.

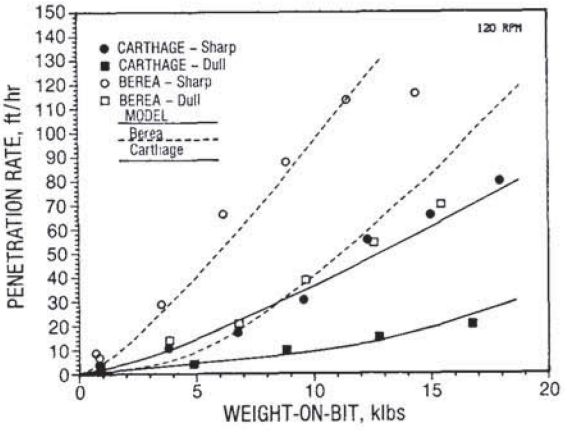

Fig. 13—Comparison of drilling rate with sharp and moderately worn bits.

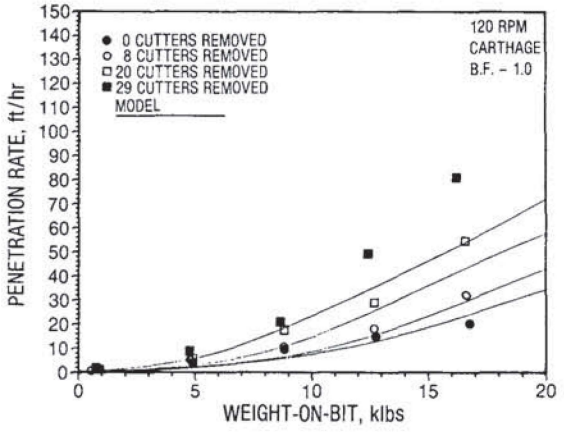

Fig. 14—Comparison of predicted and observed penetration rate for cutter removal tests with worn bit.

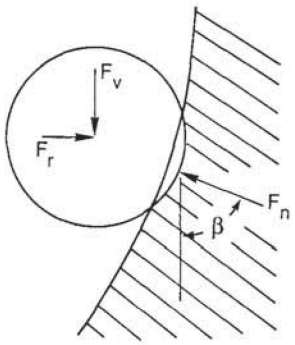

Fig. 15—Cutter on inclined surface.

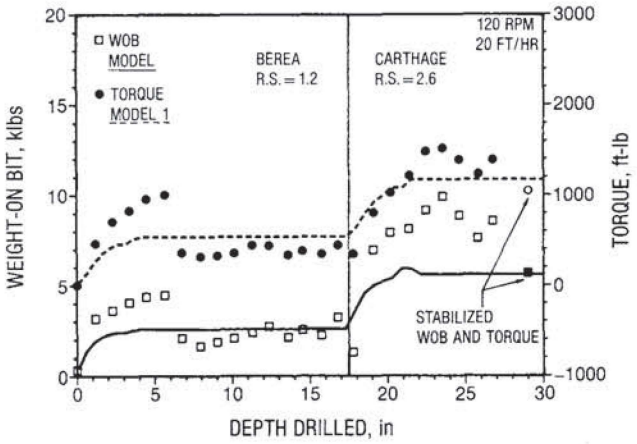

Fig. 16—Measured and predicted data while drilling through bed boundary with Bit C.

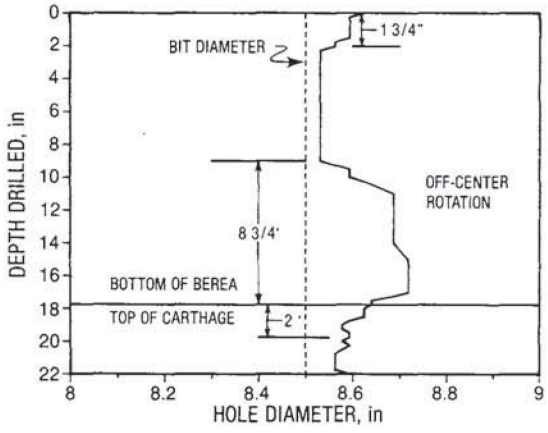

Fig. 17—Calipered hole diameter for drilling bed boundary test.

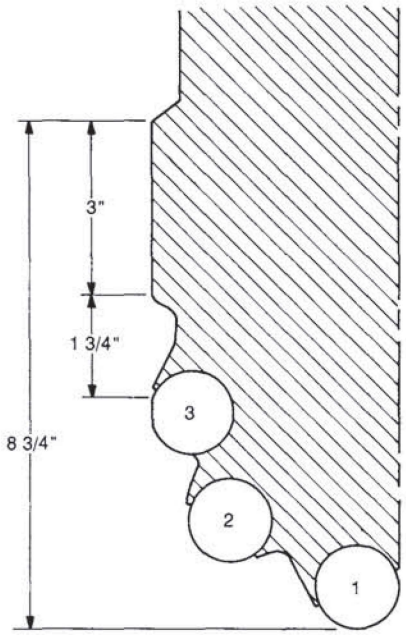

Fig. 18—Schematic of blade on Bit C used in bed boundary drilling test.

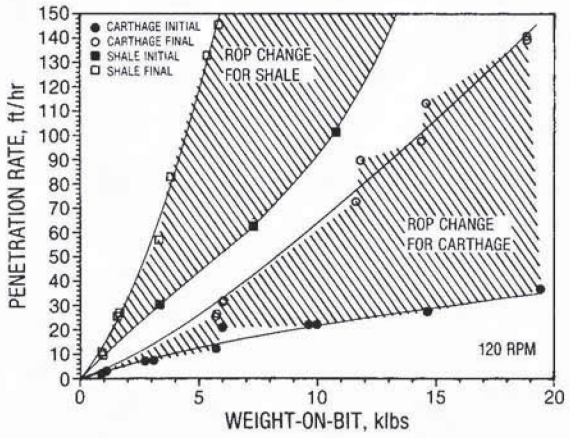

Fig. 19—Penetration rate of Bit D before and after initial wear.

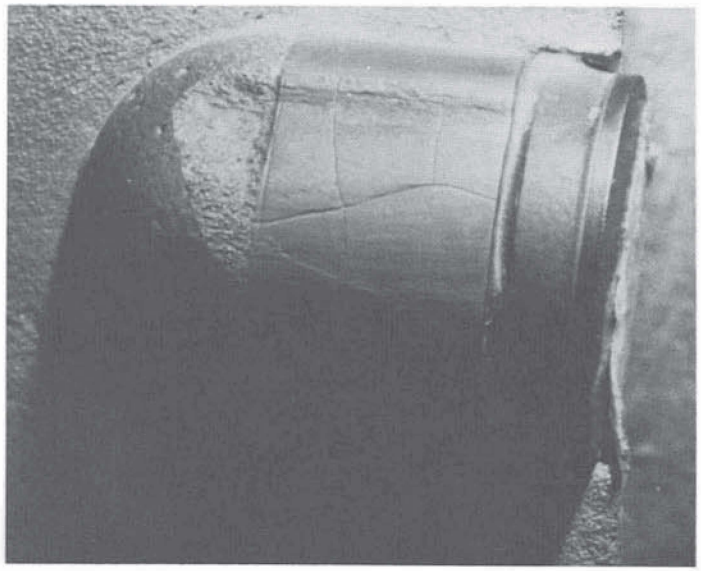

Fig. 20—Localized wear on Bit D.

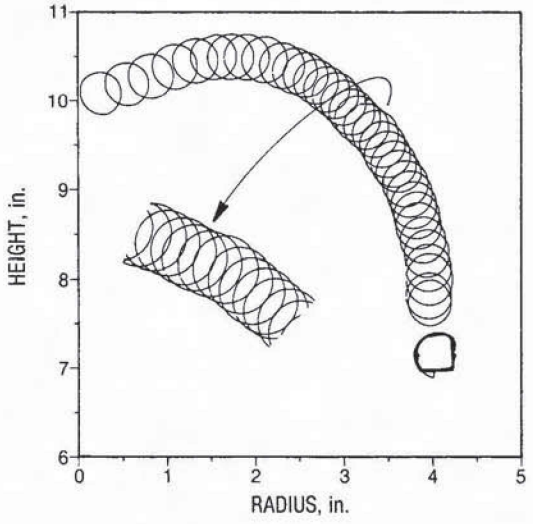

Fig. 21—Measured cutter profile of Bit D.

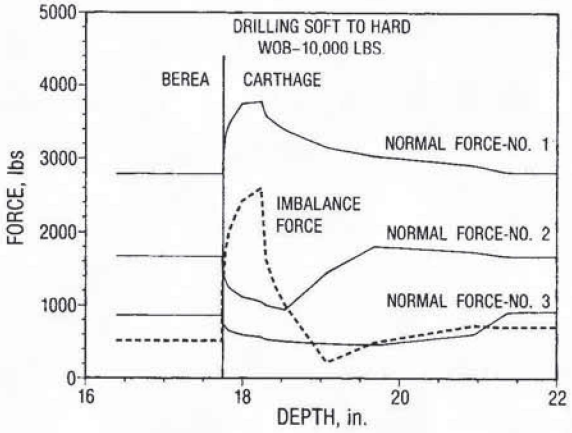

Fig. 22—Predicted cutter and imbalance forces while drilling across a bed boundary.

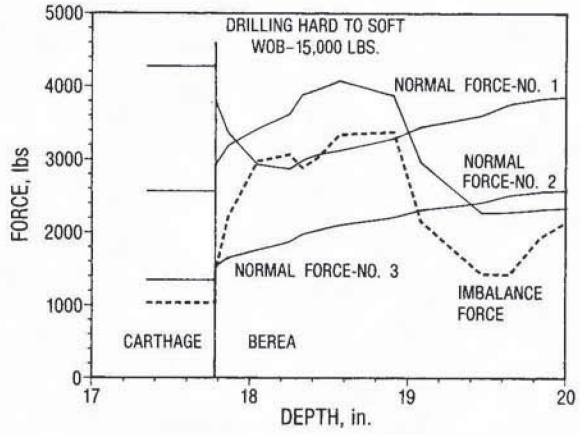

Fig. 23—Predicted cutter and imbalance forces while drilling across a bed boundary.

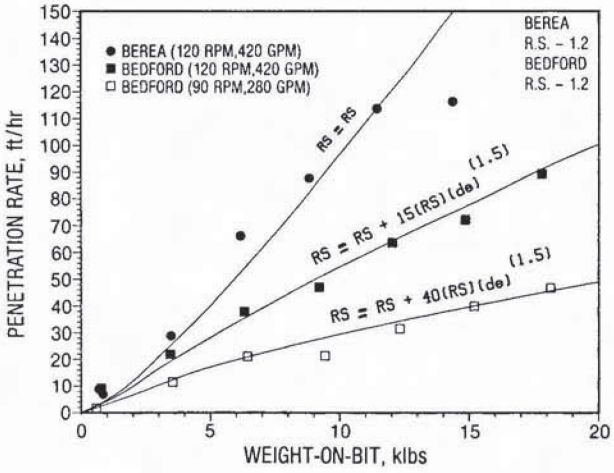

Fig. 24—Penetration rate of Bit B in Indiana limestone.

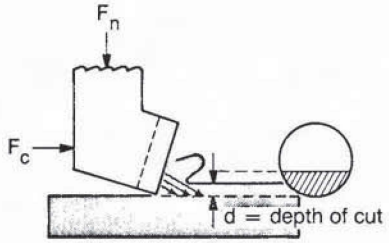

Fig. 25—Schematic of cuttings confining rock ahead of cutter.

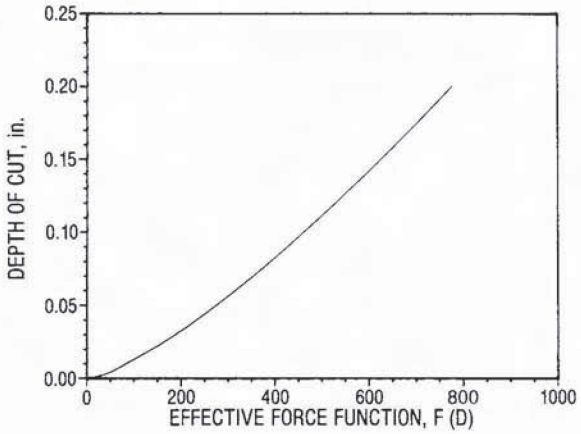

Fig. 26—Laboratory-derived effective penetrating force function.

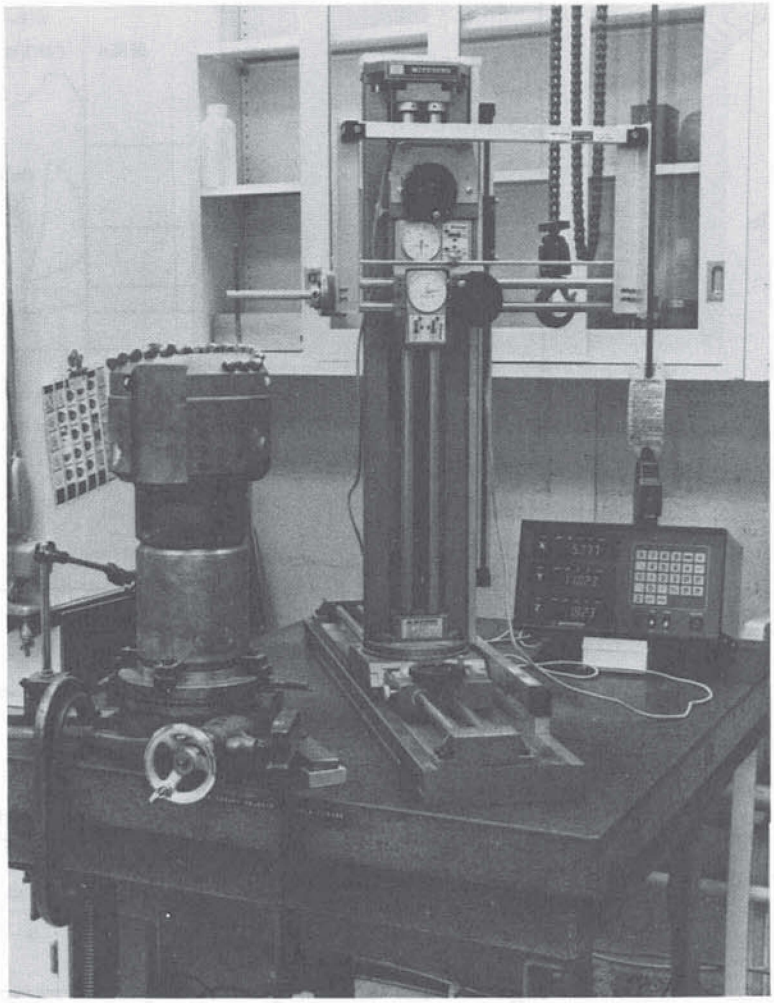

Fig. 27—Coordinate measuring machine for measuring PDC bits.

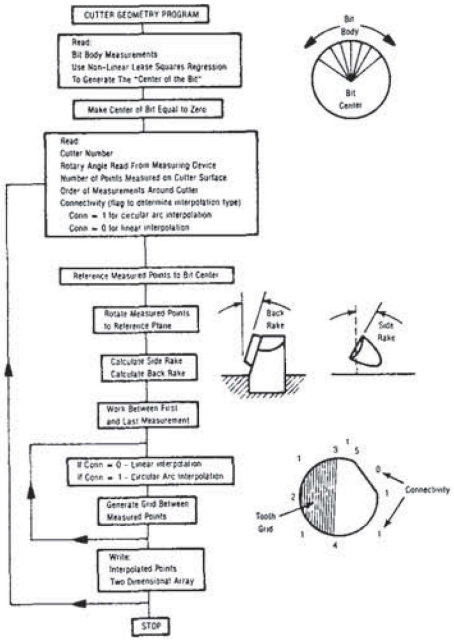

Fig. 28—Flow chart of cutter profile generation.

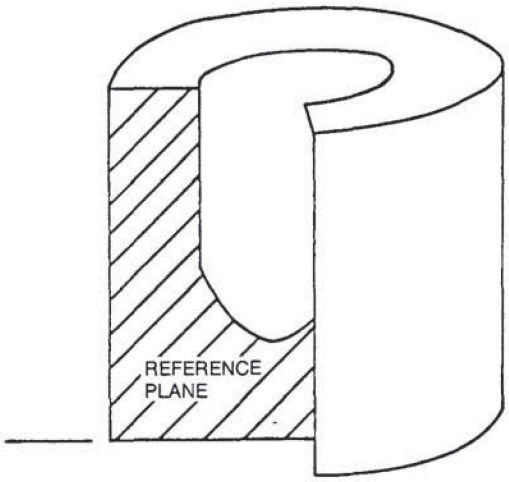

Fig. 29—Schematic of the cutting plane for PDC bit model calculations.

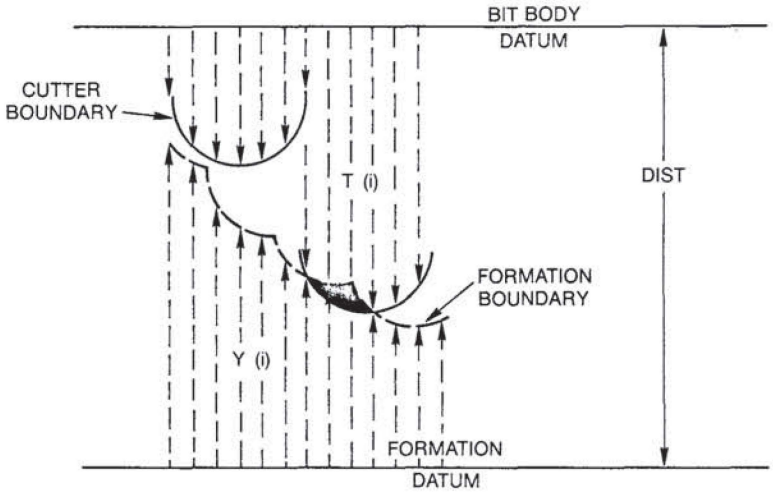

$$CUT\ (i) = T\ (i) + Y\ (i) - DIST - WEAR\ (i)$$

Fig. 30—Schematic of cutter/rock interaction for rock-removal calculations.